

ANALYTICAL METHOD FOR DETERMINING THE LOCATION OF IONOSPHERIC AND ATMOSPHERIC LAYERS FROM RADIO OCCULTATION DATA

A. G. Pavelyev,^{1*} K. Zhang,² C. S. Wang,²
Y. A. Liou,³ and Yu. Kuleshov⁴

UDC 551.051+621.396

We generalize the fundamental principle of the radio-occultation method for studying the atmospheres and ionospheres of planets and the Earth. The criterion containing the necessary and sufficient condition under which the tangential point, at which the refractive-index gradient is normal to the ray trajectory coincides with the radio-ray perigee, is obtained. The method for determining the location and parameters of ionospheric and atmospheric layers, which is based on the relationship between the amplitudes and phases of the analytic functions determined from variations in the phase path (eikonal) and intensity of the radio-occultation signal, is proposed. This method yields qualitative and quantitative estimations of the value of the spatial displacement of the ionospheric or atmospheric layer with respect to the radio-ray perigee and allows one to determine the altitude and inclination of the ionospheric layer. The developed method is, in particular, required for determining the location and inclination of the wind-shear region and the direction of propagation of internal waves in the ionosphere and the atmosphere. This method is simpler and more accurate than the back-propagation, radio-holographic method which was previously used for determining the location of the ionospheric irregularities.

1. INTRODUCTION

The radio-occultation method is widely used in two-position remote sensing, when a transmitter and a receiver move from the opposite sides with respect to the planetary limb. Since 1964, this method has successfully been used for studying the stratified structure of the planetary atmospheres ionospheres [1, 2]. With the advent of geostationary and navigation satellites, the radio-occultation experiments were started in order to study the three-dimensional structure of the Earth's ionosphere and atmosphere in the global scale [3, 4]. Use of high-stability, atomic-clock synchronized signals of navigational systems for the radio-occultation studies of the Earth's atmosphere and ionosphere has significantly increased the efficiency of the radio-occultation method whose advantages are high spatial resolution, global sounding, high accuracy, long-term stability, all-weather capability, and the possibility of almost simultaneous measurements of the atmospheric and ionospheric structures [3–7]. In terms of efficiency, the radio-occultation monitoring is comparable with global radio tomography used for remote sensing of the ionosphere by ground-based and satellite-borne means [8].

The global spherical symmetry of the ionosphere and atmosphere and the coincidence of their centers are the main conditions underlying the radio-occultation method [1–7]. Once they are fulfilled, variations

* alxndr38@mail.ru

¹ Fryazino Branch of the V. A. Kotel'nikov Institute of Radio Engineering and Electronics, Fryazino, Moscow Region, Russia; ² SPACE Research Centre, RMIT University, Melbourne, Australia; ³ Center for Space and Remote Sensing Research, National Central University, Chung-Li, Taiwan; ⁴ National Climate Centre, Bureau of Meteorology, Melbourne, Australia. Translated from *Izvestiya Vysshikh Uchebnykh Zavedenii, Radiofizika*, Vol. 55, No. 3, pp. 186–194, March 2012. Original article submitted December 8, 2011; accepted March 25, 2012.

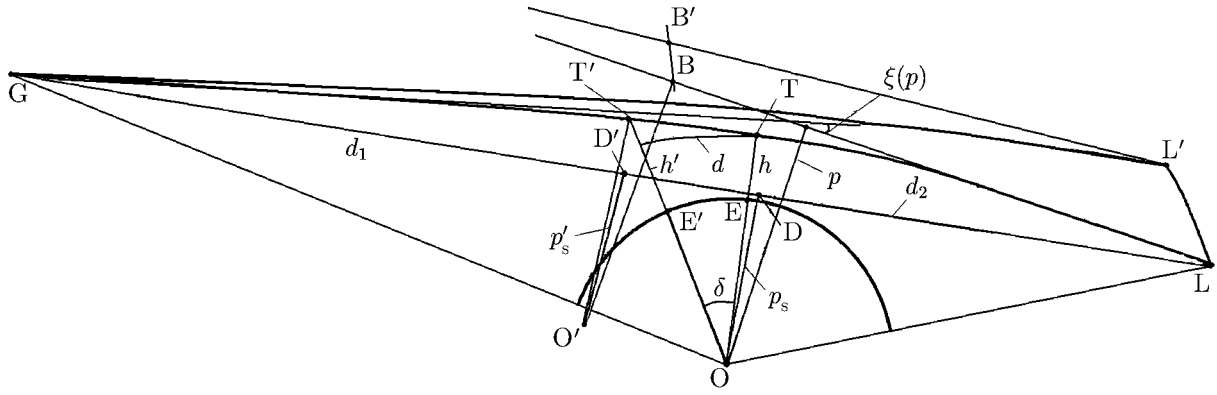


Fig. 1. Radio-occultation experimental layout.

in the vertical gradient of the refractive index in the radio-ray perigee are the main cause for variations in the amplitude and phase of a radio-occultation signal recorded by the low-orbit satellite receiver [9]. Intense frequency-dependent variations in the amplitude and phase of a radio-occultation signal, which are often observed in the height $h(T)$ interval 30–80 km of the radio-ray perigee located above the main part of the neutral atmosphere and below the ionospheric E layer, contradict the assumption of the global spherical symmetry [10]. This phenomenon is explained in [11–13] by the influence of the inclined plasma layers which are located in the ionosphere at the usual altitudes 90–130 km, but at significantly large distances from the radio-ray perigee. The back-propagation radio-holographic method was proposed in [10, 14] for determining the location of irregularities in the ionospheric E and F layers. The method for measuring the plasma-layer inclination and displacement with respect to the radio-ray perigee in the Earth's and Venus' ionospheres from the radio-occultation data, which is based on the relationship between variations in the phase-path (eikonal) acceleration and the intensity of radio-occultation signal, is proposed in [15–17].

It is the purpose of this work to obtain the criterion containing the necessary and sufficient condition of that the layer location determined from the radio-occultation experiments coincides with the radio-ray perigee and introduce the method for determining the location and measuring the characteristics of the layers from the radio-occultation data. The proposed analysis technique significantly complements the main concepts and has a general meaning for the radio-occultation measurements of three-dimensional atmospheric and ionospheric structures of the Earth and planets over a wide frequency range.

2. RADIO-OCCULTATION METHOD AND THE CRITERION FOR DETERMINING THE LAYER LOCATION

The diagram of the radio-occultation experiments is shown in Fig. 1. The high-stability radio signals radiated by satellite G pass through the ionosphere and the atmosphere along the GTL ray and are recorded by a receiver onboard another satellite L. The amplitude $A(t)$ and variations in the phase-path increase (eikonal) $\Phi(t)$ at the carrier frequency are recorded as functions of time t onboard satellite L. The global spherical symmetry of the ionosphere and the atmosphere with the common center at point O in Fig. 1 is the key assumption when analyzing the radio-occultation experiment data. During the analysis, a small region with its center at the tangential point T, where the radio ray is normal to the refractive-index gradient, makes the main contribution to the variations in amplitude and phase of a radio-occultation signal recorded by receiver L despite a significantly greater path length along the ray trajectory GTL [9]. The length of this region on the ray trajectory GTL is equal to the horizontal resolution $\Delta_h = 2(2l_f r_e)^{1/2}$ of the radio-transmission method, where $l_f = (\lambda d_2)^{1/2}$ is the Fresnel-zone size, λ is the wavelength, r_e is the TO-segment length, and d_2 is the TL-segment length, which is approximately equal to the DL-segment length (Fig. 1). The quantity of Δ_h corresponds to the minimum horizontal layer length which is measured by the radio-occultation method. Contribution of this small region to the amplitude and phase variations under the standard ionospheric conditions is much greater than that from the remaining part of the GTL path [9].

Under conditions of global spherical symmetry, the tangential point at which the GTL radio ray is normal to the refractive-index gradient coincides with the perigee T of the GTL ray trajectory. The radio-occultation method allows us to determine the refractive coefficient and its vertical gradient along the trajectory of the GTL-ray perigee with high vertical resolution and accuracy.

An important relationship between the eikonal acceleration a and the refractive attenuation $X_p(t)$ of a radio ray was obtained in [15] and has the form

$$1 - X_p(t) = ma, \quad a = d^2\Phi(t)/dt^2, \quad m = d_1 d_2 / (R_0 dp_s/dt)^2, \quad d_1 = R_0 - d_2, \quad (1)$$

where d_1 , d_2 , and R_0 are the distances along the straight lines GD, DL, and GL, respectively, while p and p_s are the impact parameters which correspond to the ray trajectory GTL and the line of sight GL. The value of m is taken from the satellite-borne observations. The distance d_2 is approximately equal to the length of the arc TL since the refractive angle $\xi(p)$ (Fig. 1) is small. In [18], it is shown that Eq. (1) is valid under the condition

$$\left| (p - p_s) \frac{dR_{1,2}}{dt} \right| \ll \left| p_s \frac{dp_s}{dt} \right|, \quad (2)$$

where R_1 and R_2 are the distances OL and OG, respectively. Equation (2) is fulfilled during the radio-occultation sensing of the atmospheres and ionospheres of the Earth and planets, since the absolute value of the difference $p - p_s$ is almost always much smaller than the impact parameters p and p_s .

Let us formulate the criterion of coincidence of the tangential point with the ray perigee. To this end, it is necessary and sufficient to require the global spherical symmetry of the atmosphere and the ionosphere and the absence of the multi-path propagation and random irregularities. Once these requirements are met and absorption is absent, Eq. (1) is valid and results in identical equality of refractive attenuations which are determined from the amplitude and phase variations of the radio-occultation signal:

$$X_p(t) \equiv X_a(t); \quad X_a(t) = I/I_0, \quad (3)$$

where I_0 and I are the radio-occultation signal intensities measured before and after the radio-ray entrance to the ionosphere, respectively. The integral absorption Γ in the atmosphere and/or ionosphere can be determined by excluding the refractive attenuation $X_p(t)$, which was found from the eikonal measurements at one frequency, with the help of Eq. (1) and the relationship $\Gamma = 1 - X_a(t)/X_p(t)$ [13, 16].

Identity (3) is the mathematical condition for finding the tangential point or the atmospheric and/or ionospheric layer in the radio-ray perigee T. It is convenient to represent variations in the refractive attenuations, which are determined from the measured variations in the eikonal and amplitude variations of the radio-occultation signal at one frequency, in the form of analytic functions having the amplitudes $A_p(t)$ and $A_a(t)$ and the phases $\chi_p(t)$ and $\chi_a(t)$:

$$1 - X_p(t) = ma = A_p(t) \operatorname{Re} \exp[j\chi_p(t)], \quad 1 - X_a(t) = ma = A_a(t) \operatorname{Re} \exp[j\chi_a(t)]. \quad (4)$$

The functions $A_p(t)$ and $A_a(t)$, and the functions $\chi_p(t)$ and $\chi_a(t)$ can be found from the known time dependences $1 - X_p(t)$ and $1 - X_a(t)$, e.g., using the numerical Hilbert transform or other methods of numerical data processing. If absorption is absent, then, under the condition of synchronous variations in the functions $1 - X_p(t)$ and $1 - X_a(t)$, we can obtain with allowance for Eq. (1) that

$$A_p(t) = A_a(t), \quad \chi_a(t) = \chi_p(t). \quad (5)$$

If the condition of the global spherical symmetry is fulfilled, then Eq. (5) represents another form of the above-mentioned criterion.

Deviations from this criterion can be related to the multi-path propagation, diffraction, scattering, and the influence of turbulence and other atmospheric and ionospheric irregularities. In some cases, these

deviations can be caused by the influence of horizontal gradients and the appearance of other tangential points in the ionospheric parts of a radio ray, e.g., the tangential point T' (Fig. 1). This leads to a displacement of the spherical-symmetry center from the point O to the point O' (Fig. 1), and Eq. (2) takes the form

$$\left| (p' - p'_s) \frac{dR'_{1,2}}{dt} \right| \ll \left| p'_s \frac{dp'_s}{dt} \right|, \quad (6)$$

where R'_1 and R'_2 are the distances $O'L$ and $O'G$, respectively.

Equation (6) is also valid in almost all practically important cases. Here, the tangential point T' coincides with the new perigee of a radio ray with respect to the center O' , and the criterion in Eq. (3) is fulfilled in the form

$$X'_p(t) \equiv X_a(t), \quad (7)$$

where $X'_p(t)$ is the refractive attenuation calculated from

$$1 - X'_p(t) = m'a, \quad a = d^2\Phi(t)/dt^2, \quad m' = d'_1 d'_2 / (R_0 dp'_s/dt)^2, \quad d'_1 = R_0 - d'_2, \quad (8)$$

where m' stands for the parameter m which corresponds to the spherical-symmetry center O' (Fig. 1), d'_2 is the distance $D'L$, and p'_s is the impact parameter which corresponds to the line of sight GL and the center O' . The first equation (7) differs from Eq. (1) by new values of the refractive attenuation $X'_p(t)$ and the factor m' for the same value of the eikonal acceleration a .

Equations (7) and (8) allow us to determine the distance d between the radio-ray perigee T and the new tangential point T' in the absence of absorption. According to Eqs. (1), (7), and (8), as well as Eq. (6), the condition of Eq. (5) should be fulfilled:

$$A'_p(t) = A_a(t), \quad \chi'_p(t) = \chi_a(t), \quad (9)$$

where $A'_p(t)$ and $\chi'_p(t)$ are the amplitude and phase of variations in the analytic representation of the refractive attenuation $1 - X'_p(t)$. By virtue of Eq. (3), the refractive attenuation obtained from the amplitude experimental data is independent of the spherical-symmetry center location. It follows from Eqs. (8) and (9) that the function $A'_p(t)$ is related to the amplitudes $A_p(t)$ and $A_a(t)$ by

$$A'_p(t) = \frac{m'}{m} A_p(t) = A_a(t); \quad A_p(t) = \frac{m}{m'} A_a(t). \quad (10)$$

If the displacement of spherical-symmetry center satisfies the conditions

$$d_2/R_0, \quad d'_2/R_0 \ll 1; \quad dp_s/dt \approx dp'_s/dt, \quad (11)$$

then the last relationship in Eqs. (10) can be written in the form

$$A_a(t) = \frac{d'_2}{d_2} A_p(t). \quad (12)$$

Equation (12) can give the following relationship for the displacement d of the tangential point T' with respect to the ray perigee T :

$$d = d'_2 - d_2 = d_2 \frac{A_a - A_p}{A_p}; \quad d_2 = \sqrt{R_2^2 - p_s^2}. \quad (13)$$

Equation (13) establishes the following rule: displacement of the tangential (turning) point of the ray trajectory is determined by the relationship between the amplitudes A_a and A_p , which are obtained from variations in the intensity and eikonal of the radio-occultation signal. The displacement d is positive (neg-

ative) depending on the sign of the difference $A_a - A_p$, while the tangential point T' in this case is located in a part of the ray trajectories GT or TL, respectively. In this case, the phases $\chi_p(t)$ and $\chi_a(t)$ should be identical within the accuracy determined by the measurement error.

Equation (13) holds when one of the satellites is located at a much greater distance from the perigee point T, than the other satellite. This condition is fulfilled when the spacecraft–Earth communication lines “are used in the radio-occultation experiments or when the low-orbit satellites working with radio signals of the space navigation systems are used. If the displacement d is known, we can determine the correction Δh to the layer height and its inclination δ with respect to the local horizon [11]

$$\delta = d/r_e, \quad \Delta h = d\delta/2, \quad (14)$$

where the parameter r_e is equal to the distance TO (Fig. 1).

The proposed method can be compared with the radio-holographic method for determining the location of the ionospheric plasma irregularities, which was introduced in [10, 14]. According to these works, to determine the radio fields between a transmitter and a receiver, the electromagnetic field measured along the orbital trajectory LL' is integrated with the Green’s function corresponding to the spherical-wave field in free space. In this case, according to the back-propagation method, the field is determined along the straight lines which are tangent to the radio-occultation ray at any point in the line LL' [14]. Using the back-propagation method, we find the region in which the amplitude modulation of an electromagnetic field is absent or minimum. The coordinates of this region determine the irregularity location. According to [21], this region is located along the phase screen (line BB' in Fig. 1), where the rays corresponding to the back-propagation field are normal to the directions laid off from the spherical-symmetry center O' (the straight lines $O'B$ and $O'B'$ in Fig. 1). The curve BB' is close to the straight line since the refractive angle is small. Inaccuracy in determining the length of the segment $T'L$ by the back-propagation method is equal to the distance between the curve BB' and the point T' : $T'B \approx p'\xi/2$ (Fig. 1). The proposed method is used for determining the layer displacement d with respect to the radio-ray perigee. Therefore, the systematic error of the introduced method is much smaller than that of the back-propagation method.

3. ANALYSIS OF EXPERIMENTAL DATA FROM THE CHAMP SATELLITE

To demonstrate the possibility of determining the plasma-layer location and inclination, we use the CHAMP satellite data, which were obtained using the radio signals from the GPS system at a frequency of 1575.42 MHz (the session of July 28, 2003 starting at 21:08 LT with the radio-ray perigee coordinates 71.4°N and 67.3°W). This data indicates the presence of intense quasi-regular amplitude and phase variations of the radio-occultation signal. The refractive attenuations X_a and X_p of the radio-occultation signals obtained by processing the intensity and eikonal variations are shown in Fig. 2a (curves 1 and 2) as functions of the perigee height h of the ray trajectory GTL. The eikonal acceleration a was determined numerically by the twofold differentiation of the second-degree polynomial which was developed by the method of least squares in the sliding time interval $\Delta t = 0.5$ s. The time interval corresponds to the vertical size of the Fresnel zone of the order of 1 km for a velocity of about 2.1 km/s of the radio-ray penetration to the ionosphere. The refractive attenuation X_p is obtained using Eq. (1) from the values of a found from the experimental data. The quantity m was taken from the data received from the satellites. The refractive attenuation X_a was determined from the amplitude data using the method of least squares with averaging over the same time interval 0.5 s.

Variations in the refractive attenuations X_a and X_p are coherent, which is indicative of the equality of the phases χ_a and χ_p . Variations in the attenuations X_a and X_p are apparently caused by the influence of three ionospheric layers in three intervals of the perigee height h of the ray trajectory GTL, which are denoted by a , b , and c in Fig. 2a. The intervals a , b , and c correspond to the height h in the ranges 50–72 km, 72–92 km, and 92–116 km, respectively. The signals $X_a - 1$ and $X_p - 1$ are coherent in the above intervals. However, the amplitudes A_a and A_p of the analytic functions $X_a - 1$ and $X_p - 1$ in these intervals are

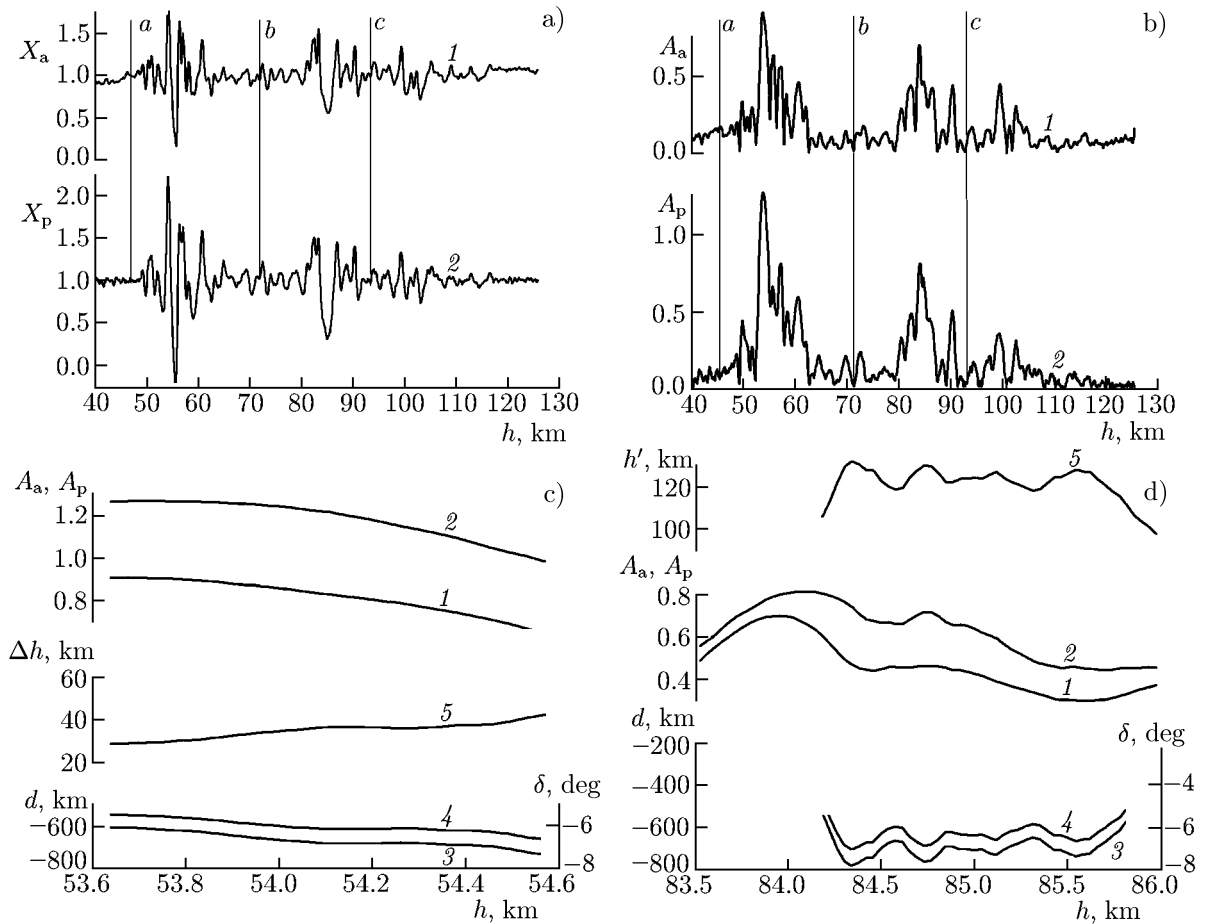


Fig. 2. Comparison of the refractive attenuations X_a and X_p , which were obtained from the variations in the intensity and eikonal of the radio-occultation signal at the frequency f_1 of the GPS system (curves 1 and 2 in panel a, respectively). The amplitude of the analytic signals corresponding to variations in the refractive attenuations X_a and X_p (curves 1 and 2 in panel b, respectively). Determination of the first-layer location using the amplitudes A_a and A_p (c). Determination of the second-layer location using the amplitudes A_a and A_p (d).

different.

The amplitudes A_a and A_p , which are determined with the help of the numerical Hilbert transform, are shown in Fig. 2b (curves 1 and 2, respectively). The amplitude A_a in the intervals a and b is smaller than the corresponding values of A_p (Fig. 2b). The opposite case is observed in the interval c (Figs. 2a and 2b). The first two layers in the intervals a and b correspond to the negative displacements d . These two layers are located on the ray trajectory GTL between the points T and L. The upper layer c is displaced from the radio-ray perigee T towards the navigation satellite G (Fig. 1).

The proposed method can be used for determining the ionospheric-layer location on the ray trajectory GTL, since variations in the refractive attenuations X_a and X_p are coherent. The results of determining the value of the displacement d in the intervals a and b are shown in Figs. 2c and 2d. Curves 1, 2, and 3 in Figs. 2c and 2d correspond to the altitude dependence of the amplitudes A_a and A_p and the displacement d , respectively. Curves 4 in Figs. 2c and 2d indicate the layer inclination δ which is shown in degrees (the right-hand vertical axis). Curves 5 represent the correction Δh to the height in kilometers (Fig. 2c) and the corrected layer height h' in kilometers (Fig. 2d), respectively.

Variations in the displacement d are concentrated in the ranges from -630 to -800 km and from -600 to -750 km (intervals a and b , respectively). The statistical error of estimating the ratio $(A_a - A_p)/A_p$ using Eq. (14) is minimum for maximum A_p . If the relative error in the measurements of A_p is 5%, then the

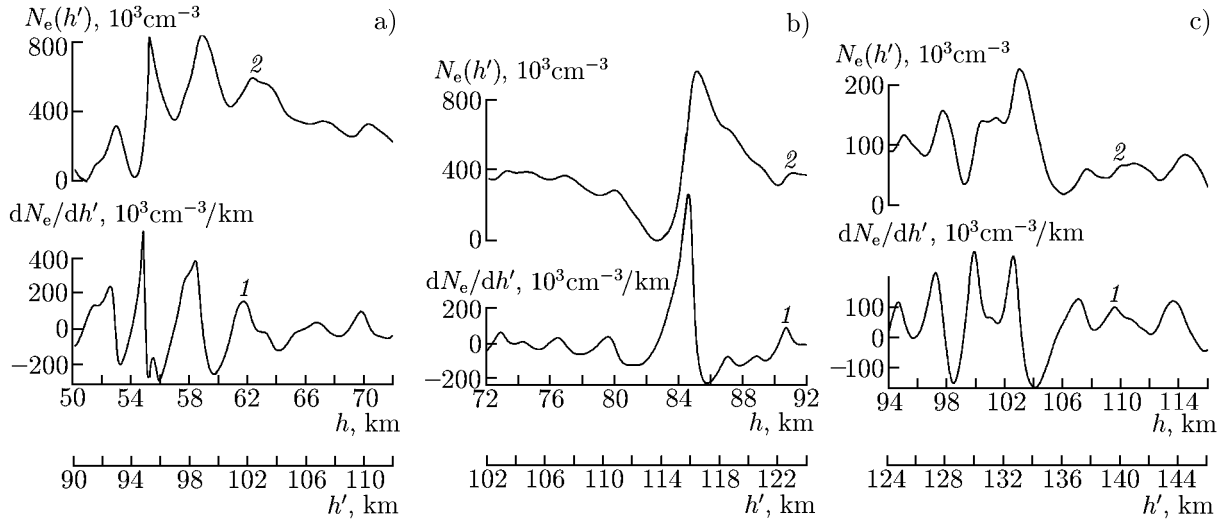


Fig. 3. Results of determining the electron number density and its vertical gradient: the parameters are $d = -730$ km and $\Delta h = 40$ km (a), $d = -640$ km and $\Delta h = 30$ km (b), and $d = 620$ km and $\Delta h = 30$ km (c).

accuracy of estimating d is about ± 100 km. The average values of the displacement in the intervals a and b are equal to $d = -730$ and $d = -620$ km, respectively. The displacement d in the interval c is positive and equals $d = 620$ km. Using Eq. (15), one can find that the inclinations of the plasma layers a , b , and c with respect to the local horizontal direction, are equal to $\delta = -7.3^\circ \pm 0.9^\circ$, $\delta = -6.4^\circ \pm 0.9^\circ$, and $\delta = 6.4^\circ \pm 0.9^\circ$, respectively.

The local spherical symmetry allows us to apply the Abel transform for solving the inverse problem and find the distribution of the electron number density and its gradient in the layer [16]. The resulting dependences of the electron number density $N_e(h')$ and its gradient dN_e/dh' are shown in Fig. 3. Curves 1 and 2 correspond to the gradient dN_e/dh' and the distribution of the electron number density N_e , which are obtained from the eikonal variations. The radio-ray perigee height h and the corrected height h' , which is determined by the above method, are shown on the upper and lower horizontal axes in Figs. 3a, 3b, and 3c, respectively.

The layers a and b are located in the segment LT at the distances from point T which are equal to approximately 730 and 620 km with the maximum electron-density gradients at the heights 95 and 117 km, respectively (curves 1 and 2 in Figs. 3a and 3b). The layer c is located in the segment GT at a distance of about 620 km from point T, while the maximum electron-density gradient is at an altitude of 130 km. According to Fig. 3, variations in the electron-density gradient in the layers a , b , and c are concentrated in the intervals

$$\begin{aligned} -2.8 \cdot 10^5 \text{ cm}^{-3}/\text{km} < dN_e(h)/dh < 5.3 \cdot 10^5 \text{ cm}^{-3}/\text{km}, \\ -2.2 \cdot 10^5 \text{ cm}^{-3}/\text{km} < dN_e(h)/dh < 7.8 \cdot 10^5 \text{ cm}^{-3}/\text{km}, \\ -2.0 \cdot 10^5 \text{ cm}^{-3}/\text{km} < dN_e(h)/dh < 3.2 \cdot 10^5 \text{ cm}^{-3}/\text{km}, \end{aligned}$$

respectively. These values are typical of the intense sporadic layers [19]. The altitude interval of the amplitude variations is approximately equal to the altitude interval of variations in the electron number density and its gradient.

According to the existing theory, the maximum of electron contact in the sporadic E layers is usually related to the location of the wind shear boundary [19]. Therefore, the radio-occultation method can be used for determining the wind-shift boundary location in the lower ionosphere. The electron-density gradient can correspond to different types of the wave fronts. In the case of internal gravity waves, the wave-vector inclination to the vertical direction can be used for finding their angular frequency [20]. Therefore, the proposed criteria and the technique extend the scope of application of the radio-occultation method.

4. CONCLUSIONS

In this paper, we have obtained an analytical criterion which allows one to determine the height, inclination, and location of the layered plasma structures by the radio-occultation method. Depending on the sign of the difference of refractive attenuations, which are obtained from the variations in the eikonal and intensity of the radio-occultation signal, the displacement of the plasma layer with respect to the radio-ray perigee is either positive or negative. In the case of global spherical symmetry of the ionosphere and the atmosphere, the radio-ray perigee point determines the layer height. The results of analysis of variations in the radio-occultation signals observed for the radio-ray perigee heights in the interval 30–90 km confirm the efficiency of the developed method for determining the layer location in the lower ionosphere. The developed technique extends the capabilities of the radio-occultation method for studying the atmospheres and ionospheres of the Earth and planets.

This work was supported by the Russian Foundation for Basic Research (project No. 10–02–01015-a) and the Presidium of the Russian Academy of Sciences (program No. 22).

REFERENCES

1. A. Kliore, D. L. Cain, G. S. Levy, et al., *Science*, **149**, 1243 (1965).
2. O. I. Yakovlev, *Cosmic Radiophysics* [in Russian], RFBR, Moscow (1998).
3. O. I. Yakovlev, V. A. Grishmanovskii, S. D. Eliseev, et al., *Dokl. Akad. Nauk SSSR*, **315**, No. 1, 101 (1990).
4. R. Ware, M. Exner, M. Gorbunov, et al., *Bull. Am. Met. Soc.*, **77**, No. 1, 19 (1996).
5. O. I. Yakovlev, A. G. Pavelyev, and S. S. Matyugov, *Satellite Monitoring of the Earth: Radio-Occultation of the Atmosphere and Ionosphere* [in Russian], URSS, Moscow (2010).
6. Y. A. Liou, A. G. Pavelyev, S. S. Matyugov, et al., *Radio Occultation Method for Remote Sensing of the Atmosphere and Ionosphere*, InTech, (2010).
7. G. Kirchengast, U. Foelsche, and A. Steiner, eds., *Occultations for Probing Atmosphere and Climate*, Springer, Berlin (2004).
8. V. E. Kunitsyn and E. D. Tereshchenko, *Ionospheric Tomography*, Springer, Berlin (2003).
9. K. Igarashi, A. Pavelyev, K. Hocke, et al., *Adv. Space Res.*, **27**, Nos. 6–7, 1321 (2008).
10. S. V. Sokolovskiy, W. Schreiner, C. Rocken, and D. Hunt, *Geophys. Res. Lett.*, **29**, No. 3, 621 (2002).
11. J. Wickert, A. G. Pavelyev, Y. A. Liou, et al., *Geophys. Res. Lett.*, **31**, No. 12, L24801 (2004).
12. A. G. Pavelyev, J. Wickert, and Y. Liou, *Radiophys. Quantum Electron.*, **51**, No. 1, 1 (2008).
13. A. G. Pavelyev, *Radiophys. Quantum Electron.*, **52**, Nos. 5–6, 363 (2009).
14. M. E. Gorbunov, A. S. Gurvich, A. V. Shmakov, *Int. J. Remote Sensing*, **23**, No. 1, 675 (2002).
15. Y. A. Liou and A. G. Pavelyev, *Geophys. Res. Lett.*, **33**, No. 23, L23102 (2006).
16. A. G. Pavelyev, Y. A. Liou, J. Wickert, et al., *Geophys. Res. Lett.*, **36**, No. 21 (2009).
17. A. G. Pavelyev, Y. A. Liou, J. Wickert, et al., *GPS Solutions*, **14**, No. 1, 3 (2010).
18. Y. A. Liou, A. G. Pavelyev, S. F. Liu, et al., *IEEE Trans. Geosci. Remote Sensing*, **45**, No. 11, 3813 (2007).
19. M. C. Kelley and R. A. Heelis, *The Earth's Ionosphere: Plasma Physics and Electrodynamics*, Elsevier Science, New-York (2009).
20. V. N. Gubenko, A. G. Pavelyev, and V. E. Andreev, *J. Geophys. Res.*, **113**, D08109 (2008)
21. V. V. Vorob'ev, A. S. Gurvich, V. Kan, et al., *Issled. Zemli Kosm.*, No. 4, 74 (1997).